

Structural Modifications of *N*-(1,2,3,4-Tetrahydronaphthalen-1-yl)-4-Aryl-1-piperazinehexanamides: Influence on Lipophilicity and 5-HT₇ Receptor Activity. Part III

Marcello Leopoldo,*[†] Enza Lacivita,[†] Paola De Giorgio,[†] Claudia Fracasso,[‡] Sara Guzzetti,[‡] Silvio Caccia,[‡] Marialessandra Contino,[†] Nicola A. Colabufo,[†] Francesco Berardi,[†] and Roberto Perrone[†]

Università degli Studi di Bari, Dipartimento Farmaco-Chimico, via Orabona, 4, 70125 Bari, Italy, Istituto di Ricerche Farmacologiche Mario Negri, via La Masa 19, 20156 Milan, Italy

Received May 23, 2008

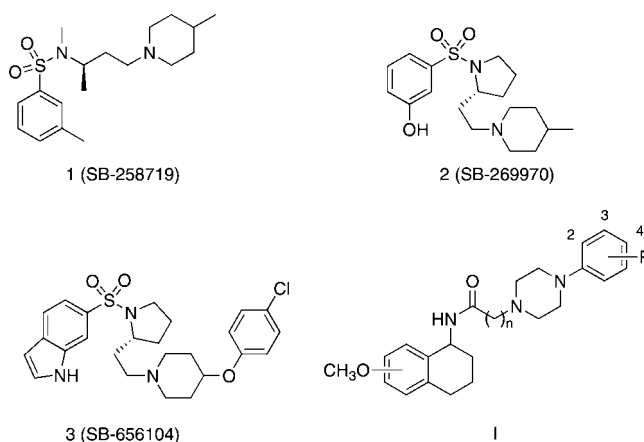
Starting from the previously reported 5-HT₇ receptor agents **4–7** with *N*-(1,2,3,4-tetrahydronaphthalen-1-yl)-4-aryl-1-piperazinehexanamide structure, the 1-(2-methylthiophenyl)-, 1-(2-diphenyl)-, 1-(2-isopropylphenyl)-, and 1-(2-methoxyphenyl)piperazine derivatives **8–31** were designed with the primary aim to obtain new compounds endowed with suitable physicochemical properties for rapid and extensive penetration into the brain. The affinities for 5-HT₇, 5-HT_{1A}, and D₂ receptors of compounds **8–31** were assessed, and several compounds displayed 5-HT₇ receptor affinities in the nanomolar range. Among these, *N*-(4-cyanophenylmethyl)-4-(2-diphenyl)-1-piperazinehexanamide (**25**) showed high 5-HT₇ receptor affinity ($K_i = 0.58$ nM), high selectivity over 5-HT_{1A} and D₂ receptors (324- and 245-fold, respectively), and agonist properties (maximal effect = 82%, $EC_{50} = 0.60$ μM). After intraperitoneal injection in mice, **25** rapidly reached the systemic circulation and entered the brain. Its brain concentration–time profile paralleled that in plasma, indicating that **25** rapidly and freely distributes across the blood–brain barrier. Compound **25** underwent *N*-dealkylation to the corresponding 1-arylpiperazine metabolite.

Introduction

Serotonin (5-hydroxytryptamine, 5-HT) controls a variety of physiological functions in the central and peripheral nervous system by interacting with a multitude of 5-HT receptor subtypes. These subtypes can be divided into seven main classes (5-HT₁ to 5-HT₇) on the basis of their pharmacological responses to specific ligands, sequence similarities at the gene and amino acid levels, gene organization, and second messenger coupling pathways. Except for the 5-HT₃ receptor, which is a ligand-gated ion channel, all serotonin receptors are coupled to G-proteins.¹

The 5-HT₇ receptor has been cloned from human, mouse, rat, guinea pig, and pig cDNA. High sequence homology (90%) has been observed between the 5-HT₇ receptors from various species, whereas a low degree of homology (40%) has been evidenced between 5-HT₇ receptor and the other G-protein coupled 5-HT receptor subtypes.² Studies in rodents on the distribution of the 5-HT₇ receptor protein in the central nervous system (CNS)^a revealed the highest abundance in thalamus, hypothalamus, and hippocampus. Within the suprachiasmatic nucleus of the hypothalamus, the 5-HT₇ receptors are located in both dendrites and axon terminals of mostly GABA containing neurons.^{3–6} Brain autoradiographic studies in human indicated that these receptors are mainly localized in the anterior thalamus and in the dentate gyrus.⁷ Irrespective of the experimental method used, there is general agreement that 5-HT₇ receptors are localized in regions of the brain involved in affective behavior and cognition and recent studies support a role for 5-HT₇ receptors in the pathogenesis of depression. In vitro binding studies in rat have also suggested that chronic

Chart 1. Structures of 5-HT₇ Receptor Agents



antidepressant treatment results in a functional downregulation of 5-HT₇-like binding sites in the hypothalamus.⁸ Studies on 5-HT₇ receptor knockout mice have displayed “antidepressant-like” phenotype in preclinical assay used to assess antidepressant potential. Also pharmacological 5-HT₇ receptor blockade by the antagonists **1** (SB-258719) or **2** (SB-269970) (Chart 1) generated robust antidepressant-like effects.^{9–13} It has been also suggested that 5-HT₇ receptor function plays a role in the control of learning and memory processes.^{14–16} Finally, pharmacological and genetic 5-HT₇ blockade has shown to partially modulate glutamatergic and dopaminergic function and therefore to be clinically useful for the treatment of positive symptoms of schizophrenia.^{17,18} In view of these outcomes, the 5-HT₇ receptor can be considered an interesting target for drug development.

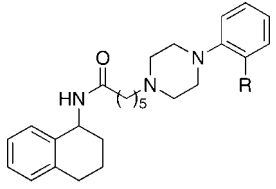
Over the last 10 years, considerable efforts have been focused on the development of novel and selective 5-HT₇ receptor agonists and antagonists.^{19,20} The first selective antagonist **1** was identified in 1997 by GlaxoSmithKline and displayed an

* To whom correspondence should be addressed. Phone: +39 080 5442798. Fax: +39 080 5442231. E-mail: leopoldo@farmchim.uniba.it.

[†] Università degli Studi di Bari.

[‡] Istituto di Ricerche Farmacologiche Mario Negri Milano.

^a Abbreviations: CNS, central nervous system; 5-CT, 5-carboxamido-tryptamine; AUC, area under the curve; 8-OH-DPAT, 8-hydroxy-*N,N*-dipropylaminotetraline.

Table 1. Physicochemical and Binding Affinities of Reference Compounds 4–7^a


compd	R	ClogP ^b	log <i>k'</i>	<i>K_i</i> , nM		
				5-HT ₇	5-HT _{1A}	D _{2L}
4 (LP-44)	SCH ₃	4.73	1.01	0.22	52.7	7.3
5 (LP-12)	Ph	6.65	1.71	0.13	60.9	224
6	CH(CH ₃) ₂	5.60	1.39	1.10	167	15
7	OCH ₃	4.78	0.63	6.64	8.6	24.6

^a Data taken from ref 28. ^b Calculated logP values (see ref 51).

arylsulfonamidoalkylamine structure, as well as compound 2, which is considered to date the standard selective 5-HT₇ receptor antagonist.²¹ However, further studies with 2 have been hampered by its rapid clearance in vivo in the rat. Years later, GlaxoSmithKline reported on the identification of the antagonist 3 (SB-656104) (Chart 1), which showed an improved pharmacokinetic profile but displayed modest selectivity over 5-HT_{2A}, 5-HT_{2B}, and 5-HT_{1D} receptors.²² The considerable amount of data on antagonists has allowed the generation of two receptor-based pharmacophores: the first containing features necessary for high 5-HT₇ receptor affinity and the other defining selectivity for this receptor subtype.²³ Considering the 5-HT₇ receptor agonists, a pharmacophore model has been generated from a set of 20 nonselective agonists.²⁴ This set included also 5-carboxamidotryptamine (5-CT), which is to date used as reference agonist.

More recently, several relatively selective 5-HT₇ agonists have been reported,^{25,26} including compounds 4 (LP-44) and 5 (LP-12) (Table 1), which were identified during our structure–activity relationship studies on a series of *N*-(1,2,3,4-tetrahydronaphthalen-1-yl)-4-aryl-1-piperazinealkylamides (structure I, Chart 1).^{27,28} Our studies indicated that for 5-HT₇ affinity: (i) a methoxy group on the 1,2,3,4-tetrahydronaphthalene ring was not essential, (ii) five methylene units separating the amide moiety and the piperazine ring were preferable, (iii) the position and the nature of the substituent on the phenyl linked to the piperazine ring was critical. In particular, we found that shifting the R substituent from the 2-position to the 3- or 4-position caused a significant loss in 5-HT₇ receptor affinity. Examination of a series of substituents in the 2-position, covering a wide range of electronic, steric, and polar properties, revealed a key role on both affinity and intrinsic activity at the 5-HT₇ receptor. Certain lipophilic substituents (R = SCH₃, CH(CH₃)₂, N(CH₃)₂, CH₃, Ph) led to high-affinity agonists, while the OH and NHCH₃ substituents switched intrinsic activity toward antagonism. The nature of this substituent was also relevant with respect to the selectivity over 5-HT_{1A} and D₂ receptors. The most relevant outcome from those studies was the identification of several high-affinity agonists (compounds 4–7, Table 1). In particular, compound 5 showed the highest selectivity among the studied derivatives. However, while studying the structure–activity relationships, we did not optimize the physicochemical properties required for penetration into the brain. It is widely accepted that brain penetration by passive diffusion becomes poor when molecular weight is larger than 450 Da, the logP is greater than 5.0, the number of hydrogen bond donors is greater than five, or when the sum of all nitrogens and oxygens is greater than 10.^{29–31} As reported in Table 1, the lipophilicity of compound

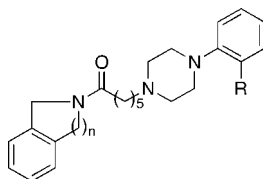
5 (ClogP = 6.65) exceeds the guideline value and this could limit its use in vivo. Keeping in mind that compound 5 was the most selective 5-HT₇ derivative, we selected also as reference the compounds 4, 6, and 7 (Table 1) because they displayed high affinity at 5-HT₇ receptor and different selectivity profiles over 5-HT_{1A} and D₂ receptors. Therefore, we targeted structural modifications on compounds 4–5 to obtain the new derivatives 8–31, which showed ClogP values within the desired range (Tables 2 and 3).

Chemistry

The synthesis of the final compounds 8–31 required the starting amines 32a,b and 36a–d (Scheme 1). Among these, only amine 36d was not commercially available; therefore, it was prepared as follows: 4-hydroxybenzylamine hydrochloride³² was first *N*-BOC protected, then was reacted with methanesulfonyl chloride to give derivative 35. Deprotection of the latter gave the benzyl amine 36d. The amines 32a,b and 36a–d reacted with 6-bromohexanoyl chloride to give the corresponding bromoalkyl derivatives 33a,b and 37a–d. Condensation of 33a,b and 37a–d with the appropriate 1-arylpiperazine gave the desired compounds 8–31.

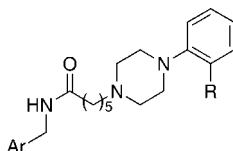
Results and Discussion

In view of the increasing interest in the development of 5-HT₇ receptor agonists, we decided to expand our structure–activity relationship studies on *N*-(1,2,3,4-tetrahydronaphthalen-1-yl)-4-aryl-1-piperazinealkylamide derivatives in order to optimize their 5-HT₇ affinity and selectivity and to explore their potential for in vivo pharmacological studies. Because a major determinant of the activity of centrally acting drugs is the rate and extent to which they enter the brain, we targeted structural modifications on compounds 4–7 to obtain the new derivatives 8–31, which had suitable ClogP values for rapid penetration into the brain. The structural modifications were performed taking into account our previous structure–activity relationship findings. We evidenced in this class of the compounds (Structure I, Chart 1) and also for other arylpiperazine-based 5-HT₇ receptor ligands^{33,34} that even limited structural changes on the 1-arylpiperazine moiety could reflect in a great variation of 5-HT₇ receptor affinity. The highest values of affinity at 5-HT₇ receptor were shown by compounds with five methylenes. For these reasons, we did not modify the arylpiperazine moiety and the alkyl chain length of compounds 4–7. Therefore, we reasoned on the possibility to reduce the lipophilicity of the terminal fragment of compounds 4–7 by replacing the tetrahydronaphthalene nucleus with three structurally related moieties (isoindoline, tetrahydroisoquinoline, benzyl) that would have less impact on the lipophilicity of the target molecules. As shown in Tables 2 and 3, compounds 8–19 displayed lower ClogP values than their corresponding tetrahydronaphthalene counterparts 4–7. However, the benzyl derivative 17 showed a ClogP of 5.28, which is quite above the guideline value. With the aim to obtain a reduction of the lipophilicity, the benzyl group attached to the amide nitrogen was therefore replaced by more polar groups such as 4-pyridinylmethyl, 4-cyanophenylmethyl, and 4-methanesulfonylphenylmethyl. This structural modification was performed on benzyl derivatives 16–19, leading to compounds 20–31 (Table 3). The actual reduction of lipophilicity of the new molecules was confirmed by determining the retention factor log *k'* as lipophilicity index by using a reversed-phase HPLC method.³⁵ Binding affinities for the rat cloned 5-HT₇ receptor were determined by radioligand displacement assay using the condition summarized in the Experimental

Table 2. Physicochemical and Binding Affinities of Compounds **8–15**

compd	n	R	ClogP	log <i>k'</i>	<i>K_i</i> , nM ± SEM ^a		
					5-HT ₇	5-HT _{1A}	D ₂
8	1	SCH ₃	2.89	1.12	42 ± 3.7	1.07 ± 0.05	96 ± 6
9	1	Ph	4.41	1.65	8.3 ± 2.1	124 ± 20	93 ± 2
10	1	CH(CH ₃) ₂	3.76	1.55	54 ± 4	22 ± 0.5	65 ± 5
11	1	OCH ₃	2.35	0.76	179 ± 15	3.2 ± 0.8	730 ± 50
12	2	SCH ₃	3.45	1.18	32.9 ± 2.1	2.04 ± 0.50	40 ± 8
13	2	Ph	4.97	1.68	3.81 ± 0.5	95 ± 5	362 ± 75
14	2	CH(CH ₃) ₂	4.32	1.61	6 ± 0.4	3.7 ± 0.8	1.3 ± 0.3
15	2	OCH ₃	2.91	0.75	31 ± 3.0	40 ± 4.5	22 ± 4
5-CT					0.50 ± 0.08		
8-OH-DPAT						2.1 ± 0.4	
haloperidol							4.2 ± 0.6

^a The values are the means ± SEM from three independent experiments with samples in triplicate.

Table 3. Physicochemical and Binding Affinities of Compounds **16–31**

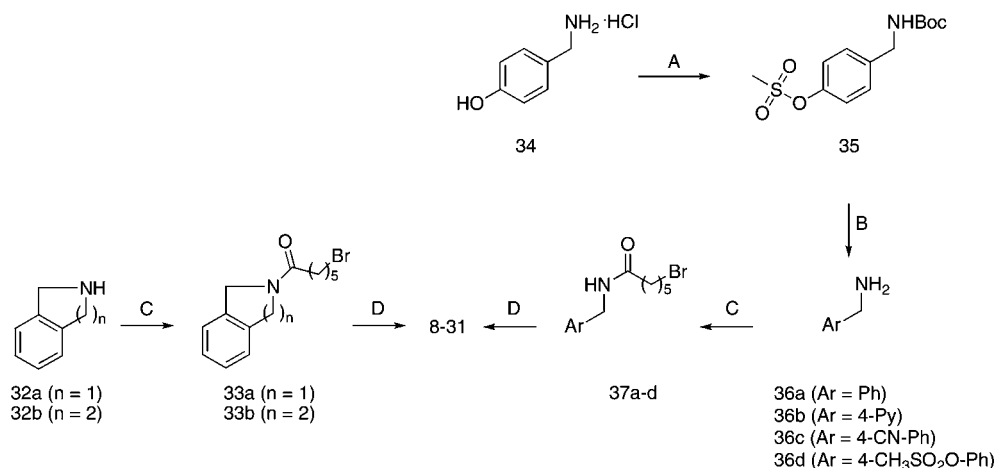
compd	Ar	R	ClogP	log <i>k'</i>	<i>K_i</i> , nM ± SEM. ^a		
					5-HT ₇	5-HT _{1A}	D ₂
16		SCH ₃	3.76	0.88	22 ± 1.5	12 ± 2.0	33 ± 5.0
17		Ph	5.28	1.39	ND ^b	161 ± 15	503 ± 70
18		CH(CH ₃) ₂	4.63	1.28	215 ± 8	139 ± 18	9.2 ± 0.8
19		OCH ₃	3.22	0.44	224 ± 15	13 ± 1.2	226 ± 30
20		SCH ₃	2.26	0.47	34.8 ± 2.1	8.2 ± 0.7	64 ± 4
21		Ph	3.78	0.96	0.98 ± 0.05	70 ± 6	185 ± 30
22		CH(CH ₃) ₂	3.13	0.89	5.1 ± 0.4	325 ± 20	21 ± 2
23		OCH ₃	1.73	0.12	389 ± 10	19 ± 3.5	501 ± 25
24		SCH ₃	3.19	0.65	9.0 ± 2.0	94 ± 4	5.3 ± 1.5
25		Ph	4.71	1.18	0.58 ± 0.02	188 ± 12	142 ± 10
26		CH(CH ₃) ₂	4.06	0.72	8.6 ± 0.5	53 ± 5	20 ± 2.5
27		OCH ₃	2.66	0.28	296 ± 15	43 ± 2.5	311 ± 18
28		SCH ₃	2.87	0.71	148 ± 20	10.3 ± 2.5	30 ± 4
29		Ph	4.39	1.08	5.7 ± 0.4	106 ± 10	723 ± 10
30		CH(CH ₃) ₂	3.74	0.92	76 ± 4	57 ± 8	7.8 ± 0.4
31		OCH ₃	2.33	0.11	71 ± 3.5	29 ± 3	91 ± 8

^a The values are the means ± SEM from three independent experiments with samples in triplicate. ^b Not detectable (see ref 34).

Section. Hill plot slope of all compounds (except **17**) were close to unity, indicating a competitive-type interaction between the tested compounds and [³H]LSD. The analysis of the *K_d* shift obtained by compound **17** resulted in a linear plot with a slope significantly different from unity, suggesting an allosteric

interaction between compound **17** and [³H]LSD under the experimental conditions used here.³⁶

The 5-HT₇ receptor affinities of target compounds **8–31** are listed in Tables 2 and 3. Considering isoindolines **8–11**, isoquinolines **12–15**, and benzyl derivatives **16–19**, one can

Scheme 1^a

^a Reagents: (A) (i) (BOC)₂O, Et₃N; (ii) methanesulfonyl chloride, Et₃N. (B) TFA. (C) 6-Bromohexanoyl chloride, 1.2% aqueous NaOH. (D) 1-Arylpiperazine.

observe a reduction in 5-HT₇ affinity as compared to the corresponding tetrahydronaphthalenyl derivatives **4–7**. In particular, the isoquinoline derivatives showed less marked lowering than the isoindoline and benzyl derivatives. The reduction was particularly evident for 2-methylthio derivatives **8**, **12**, and **16** and for derivative **18** (≥100-fold), whereas compounds **9**, **13**, and **14** retained affinity values in the nanomolar range. Plotting the p*K*_is against ClogP values of compounds **4–19** revealed a low correlation coefficient (data not shown), suggesting that the apolar nature of the terminal fragment is not the only feature that modulates the interaction of this part of the ligand with the 5-HT₇ receptor. To some extent, this observation was confirmed by comparing 5-HT₇ receptor affinity data of derivatives **16**, **18**, and **19** with those of their less lipophilic analogues **20**, **22–24**, **26–28**, **30**, **31** (Table 3). In fact, replacement of the benzyl group attached to the amide nitrogen by more polar groups had a limited impact on 5-HT₇ affinity, except for **22** and **26**, which were 42- and 25-fold more potent than **18**. It is interesting to note that the presence of 4-pyridinylmethyl, 4-cyanophenylmethyl, and 4-methanesulfonylphenylmethyl as a terminal fragment was also well tolerated in the case of 2-phenyl derivatives **21**, **25**, and **29**, which showed high 5-HT₇ affinity (5.7 nM < *K*_i < 0.58 nM).

The affinities for 5-HT_{1A} and D₂ receptors of the target compounds were also assessed because they may interfere with the evaluation of pharmacological actions mediated by 5-HT₇ receptors (i.e., body temperature, sleep patterns).^{37,38} The structural simplification of the tetrahydronaphthalene nucleus of **4–7** did not cause great variations in 5-HT_{1A} affinity. The isoquinoline, isoindoline, and benzyl derivatives **8–19** showed *K*_i values that differed at least 10-fold from the parents **4–7**, except **12**, which was about 26-fold more potent than **4**. These data indicated that, within this class of arylpiperazine-based ligands, the affinity at 5-HT_{1A} receptor is marginally affected by the nature of the terminal fragment. A similar trend was shown by affinity data at dopamine D₂ receptor: *K*_i values of isoindolines **8–11**, isoquinolines **12–15**, and benzyl derivatives **16–19** were within 1 order of magnitude as compared to tetrahydronaphthalenyl counterparts **4–7**. This binding profile was replicated by derivatives **20–31**, which showed even smaller variation of affinity at both 5-HT_{1A} and D₂ receptors. As a result of the above-discussed trend of affinity at 5-HT₇, 5-HT_{1A}, and D₂ receptors, the specificity for 5-HT₇ receptor of the new compounds **8–31** was, at best, unchanged as compared to the reference compounds **4–7**. From these data, it became

Table 4. Relaxation Effect Induced by Selected Compounds and 5-CT on Substance P-Stimulated Guinea Pig Ileum Contracture

compd	% max activity ^a	EC ₅₀ , μM	pA ₂ of compd 2 ^b
5 ^c	74	1.77 ± 0.08	7.84 ± 0.20
13	89	0.49 ± 0.03	7.80 ± 0.20
21	87	0.31 ± 0.08	7.96 ± 0.20
25	82	0.60 ± 0.04	7.69 ± 0.20
5-CT	100	0.63 ± 0.04	7.48 ± 0.12

^a Percentage of the relaxation effect mediated by 5-HT₇ receptors. ^b pA₂ values of the standard antagonist **2** determined by using the corresponding agonist. ^c Data taken from ref 28.

apparent that maintaining potency and selectivity for the biochemical target while optimizing the physicochemical properties is a complex challenge. Nonetheless, the 2-phenyl derivatives **13**, **21**, and **25** showed appreciable selectivity (25- to 324-fold over 5-HT_{1A} and 95- to 245-fold over D₂ receptors), still retaining nanomolar affinity at 5-HT₇ receptor and showing lipophilicity within the target range. These ligands were further characterized for their intrinsic activity at 5-HT₇ receptor by measuring the 5-HT₇ agonist mediated relaxation of substance P-induced contraction in an isolated guinea pig ileum assay (Table 4). They showed full competitive agonism at 5-HT₇ receptor, being that their effect abolished dose-dependently by the selective 5-HT₇ antagonist **2**. In particular, compounds **21** and **25** demonstrated EC₅₀ values comparable to that of the standard 5-HT₇ agonist 5-CT and higher potency than the tetrahydronaphthalenyl derivative **5**. It can be noted that the modification of the terminal fragment of **5** left unchanged the intrinsic activity of **13**, **21**, and **25**, confirming the predominant role of the arylpiperazine moiety on the intrinsic activity in this class of compounds.

On the basis of its affinity for the 5-HT₇ receptor (*K*_i = 0.58 nM), selectivity over 5-HT_{1A} and D₂ receptors (324- and 245-fold, respectively), and intrinsic activity profile (maximal effect = 82%, EC₅₀ = 0.60 μM), compound **25** (LP-211) was injected in male mice (10 mg/kg) to preliminarily determine its distribution between blood and brain and thus find out to what extent it passes the blood–brain barrier and the concentrations reached at the site of action. Moreover, the potential formation of 1-(2-diphenyl)piperazine and its brain-to-plasma concentration ratio were also examined because arylpiperazine derivatives generally undergo *N*-dealkylation of the aliphatic chain attached to the piperazine nitrogen.³⁹ Similar studies were performed on compound **4**, which has a lipophilicity comparable with **25**. As shown in Figure 1, compound **25** rapidly reached the systemic

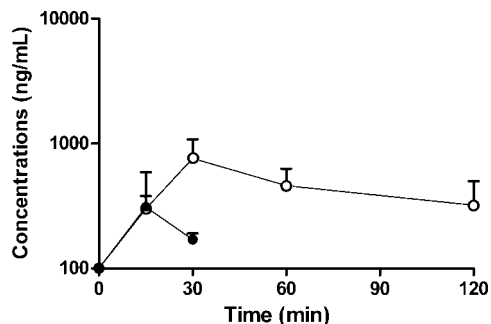


Figure 1. Plasma concentration–time curves of compounds **25** (open symbols) and **4** (closed symbols) after intraperitoneal injection in mice (10 mg/kg; $N = 3$).

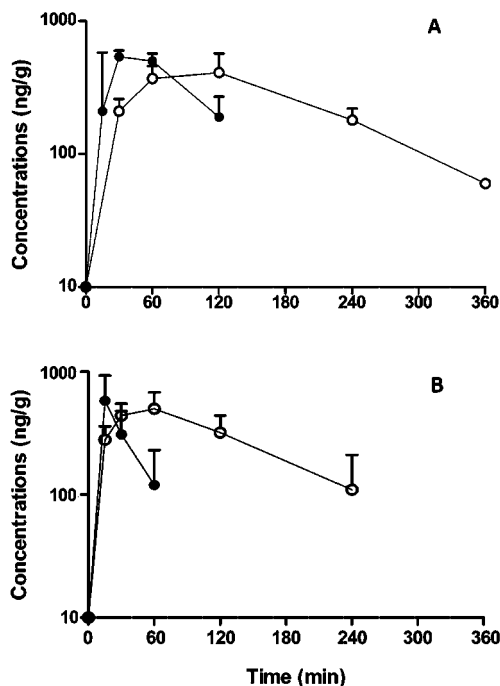


Figure 2. Brain concentration–time curves of compounds **25** (A) and **4** (B) after intraperitoneal injection in mice (10 mg/kg). Each value is the mean of 3 mice for the parent compound (closed symbols) and their 1-aryl-piperazine metabolite (open symbols).

circulation in the mouse, achieving mean C_{\max} of $0.76 \pm 0.32 \mu\text{g/mL}$ at 30 min, with quantifiable levels consistently evident for up to 2 h. Under the assumption of complete absorption of this derivative from the injection site into the systemic circulation, the mean total body clearance approached liver blood flow. In conjunction with a relatively high volume of distribution of about 11 L/kg, this resulted in a mean elimination half-life of 65 min. In the same experimental conditions, compound **4** reached plasma C_{\max} ($0.31 \pm 0.07 \mu\text{g/mL}$) at the first sampling time (15 min). It was then cleared rapidly, with plasma concentrations approximately halving after 30 min, and the compound was no longer measurable in mouse plasma after 1 h ($<0.1 \mu\text{g/mL}$, using 0.1 mL of plasma). In both cases, the plasma concentrations of their 1-arylpiperazine metabolite were always below the detection limit of the analytical procedure, at this dose of **25** and **4**.

Reflecting the time profile in the systemic circulation, compound **25** achieved mean brain C_{\max} at approximately the same time as in plasma, i.e., 30 min after dosing (Figure 2A). Mean C_{\max} averaged $0.54 \pm 0.06 \mu\text{g/g}$. These concentrations then declined almost parallel with plasma concentrations,

yielding a mean brain-to-plasma distribution ratio (plasma/brain AUC) of about 0.7. Compound **4** too peaked in brain at approximately the same time as in plasma (Figure 2B), but mean C_{\max} ($0.58 \pm 0.35 \mu\text{g/g}$) was about twice that in plasma, looking at the whole brain concentrations. However, the low and short-lasting compound levels did not allow an accurate determination of the terminal $t_{1/2}$, although a rough estimate suggested that, at least at this dose, compound **4** was less persistent in the brain than compound **25** (elimination $t_{1/2}$ about 20 and 69 min, respectively). Unlike plasma concentrations, brain concentrations of 1-(2-diphenyl)piperazine (Figure 2A) rose rapidly and reached C_{\max} of $0.41 \pm 0.06 \mu\text{g/g}$ within 120 min for compound **25**, then declined with an elimination $t_{1/2}$ of 87 min. Mean AUC was $94 \mu\text{g/mL} \cdot \text{min}$, yielding a metabolite-to-parent compound ratio of about 1.6. Similarly, the metabolite of compound **4**, 1-(2-methylthiophenyl)piperazine, appeared rapidly in mouse brain ($C_{\max} = 0.50 \pm 0.11 \mu\text{g/g}$, at 60 min), disappearing thereafter at a slower rate (elimination $t_{1/2}$ about 82 min) than the parent compound (Figure 2B). The AUC of 1-(2-methylthiophenyl)piperazine ($85 \mu\text{g/mL} \cdot \text{min}$) exceeded that of its parent compound by about 4.1 times. This was not surprising, as previous studies have shown that 1-arylpiperazines concentrate in brain tissue, achieving concentrations several times those in the blood.³⁹ This is probably related to their lipophilicity, which leads to the extensive uptake into lipid-containing tissue.⁴⁰

Conclusions

In summary, we have described the synthesis of the new 1-arylpiperazine-based derivatives **8–31**. These compounds originated from the structural simplification of the previously reported 5-HT₇ receptor agents **4–7** with *N*-(1,2,3,4-tetrahydronaphthalen-1-yl)-4-aryl-1-piperazinehexanamide structure. The affinities of derivatives **8–31** for 5-HT₇ receptor as well as those for serotonin 5-HT_{1A} and dopamine D₂ were assessed by radioligand binding assays. The proposed structural modifications on the tetrahydronaphthalenyl ring of compounds **4–7** were, in most cases, detrimental for 5-HT₇ receptor, whereas they had limited impact on the affinity for 5-HT_{1A} and D₂ receptors. Nonetheless, the pursued strategy led to the identification of the 1-(2-diphenyl)piperazine derivatives **13**, **21**, and **25**, which retained nanomolar affinity at 5-HT₇ receptor, appreciable selectivity (25- to 324-fold over 5-HT_{1A} and 95- to 245-fold over D₂ receptors), still showing lipophilicity within the target range. Compounds **13**, **21**, and **25** showed full competitive agonism at 5-HT₇ receptor in an isolated guinea pig ileum assay, as well as their corresponding tetrahydronaphthalenyl derivative **5**. Compound **25** rapidly crossed the blood–brain barrier and equilibrated with plasma, achieving concentrations in the low micromolar range after intraperitoneal doses in mice. Compound **25** undergoes *N*-dealkylation of the aliphatic chain attached to the piperazine nitrogen, resulting in the formation of 1-(2-diphenyl)piperazine, whose pharmacokinetic behavior is different from the parent compound. Future studies will focus on characterization of the neuropharmacological profile of this metabolite compared with compound **25**.

Experimental Section

Chemistry. Column chromatography was performed with 1:30 Merck silica gel 60A (63–200 μm) as the stationary phase. Melting points were determined in open capillaries on a Gallenkamp electrothermal apparatus. Elemental analyses (C, H, N) were performed on Eurovector Euro EA 3000 analyzer; the analytical results were within $\pm 0.4\%$ of the theoretical values for the formula given. ¹H NMR spectra were recorded at 300 MHz on a Varian Mercury-VX spectrometer. All spectra were recorded on free bases.

All chemical shift values are reported in ppm (δ). Recording of mass spectra was done on an HP6890–5973 MSD gas chromatograph/mass spectrometer; only significant m/z peaks, with their percentage of relative intensity in parentheses, are reported. ESI⁺/MS/MS analysis were performed with an Agilent 1100 Series LC-MSD trap System VL workstation. All spectra were in accordance with the assigned structures. The purity of new compounds that were essential to the conclusions drawn in the text were determined by HPLC on a Perkin-Elmer Series 200 LC instrument using a Phenomenex Prodigy ODS-3 RP-18 column, (250 mm \times 4.6 mm, 5 μ m particle size) and equipped with a Perkin-Elmer 785A UV/vis detector setting $\lambda = 254$ nm. Compounds **8–31** were eluted with CH₃OH/H₂O/Et₃N, 4:1:0.01, v/v, at a flow rate of 1 mL/min. When necessary, a standard procedure was used to transform final compounds into their hydrochloride salts. The following compounds were synthesized according to published procedures: 4-hydroxybenzylamine,³² 1-(2-isopropylphenyl)piperazine,⁴¹ 1-(2-diphenyl)piperazine.⁴²

***N-t*-Butoxycarbonyl-4-(methanesulfonyloxyphenyl)methanamine (35)**. 4-Hydroxybenzylamine hydrochloride (3.18 g, 14.7 mmol) was solubilized in a mixture of H₂O (25 mL) and THF (60 mL). Et₃N (2.16 mL, 14.7 mmol) and di-*t*-butylcarbonate (3.4 g, 14.7 mmol) was added to the solution. The mixture was stirred at room temperature overnight. Then THF was evaporated in vacuo and the aqueous residue was extracted with AcOEt (3 \times 20 mL). The organic phases were collected, dried over Na₂SO₄, and concentrated under reduced pressure. The crude residue was chromatographed (CHCl₃/AcOEt 9:1 as eluent) to give the Boc protected amine as a yellow solid. Triethylamine (2.5 mL, 17.9 mmol) and methanesulfonyl chloride (1.5 mL, 19.4 mmol) were added to a solution of Boc protected amine (2.7 g, 12.1 mmol) in CH₂Cl₂ cooled at -10 °C. The mixture was stirred at room temperature for 6 h. Then, the reaction mixture was first washed with a saturated aqueous solution of NaHCO₃ and then with 3 N HCl. The separated organic phase was dried over Na₂SO₄ and concentrated under reduced pressure to yield pure **35** as a white semisolid (2.8 g, 77% yield). ¹H NMR (CDCl₃): δ 1.45 (s, 9H), 3.13 (s, 3H), 4.31 (br d, 2H), 7.21–7.25 (m, 2H), 7.33 (d, 2H, $J = 8.5$ Hz).

4-Methanesulfonyloxyphenylmethanamine (36d). A mixture of **35** (1.4 g, 4.65 mmol) and trifluoroacetic acid (1.04 mL, 14 mmol) in CH₂Cl₂ (30 mL) was stirred at room temperature overnight. Then the reaction mixture was washed twice with aqueous 20% Na₂CO₃ (2 \times 20 mL). The organic phase was separated, dried over Na₂SO₄, and evaporated under reduced pressure, giving pure **36d** as a yellow oil (0.78 g, 83% yield). ¹H NMR (CDCl₃): δ 2.12 (s, 2H, D₂O exchanged), 3.07 (s, 3H), 3.82 (s, 2H), 7.15–7.19 (m, 2H), 7.25–7.33 (m, 2H).

General Procedure for Preparation of Alkylating Agents 33a,b and 37a–d. A cooled solution of amine **32a,b** and **36a–d** (4.0 mmol) in CH₂Cl₂ was stirred vigorously with 2% aqueous NaOH (9.6 mL, 4.8 mmol) while 6-bromohexanoyl chloride (4.8 mmol) in CH₂Cl₂ was added dropwise. The same NaOH solution was then used to maintain pH at 9, and at constant pH the layers were separated. The organic phase was washed with 3 N HCl, with H₂O, and then dried over Na₂SO₄ and evaporated under reduced pressure. The crude residue was chromatographed as detailed below to give compounds **33a,b** and **37a–d** as white semisolids.

***N*-(6-Bromo-1-oxohexyl)isoindoline (33a)**. Eluted with CHCl₃/AcOEt, 9:1; 80% yield. ¹H NMR (CDCl₃): δ 1.48–1.59 (m, 2H), 1.71–1.81 (m, 2H), 1.87–1.97 (m, 2H), 2.40 (app t, 2H), 3.43 (t, 2H, $J = 6.8$ Hz), 4.80 (s, 4H), 7.24–7.31 (m, 4H). GC/MS: m/z 297 (M⁺ + 2, 32), 295 (M⁺, 32), 216 (32), 161 (68), 160 (64), 146 (43), 118 (100).

***N*-(6-Bromo-1-oxohexyl)-1,2,3,4-tetrahydroisoquinoline (33b)**. Eluted with CHCl₃/AcOEt 9:1; 90% yield. ¹H NMR (CDCl₃): δ 1.46–1.56 (m, 2H), 1.66–1.76 (m, 2H), 1.85–1.95 (m, 2H), 2.42 (app t, 2H), 2.83–2.92 (m, 2H), 3.39–3.44 (m, 2H), 3.38 (t, 1H, $J = 5.8$ Hz), 3.83 (app t, 1H), 4.62 (s, 1H), 4.73 (s, 1H), 7.09–7.23 (m, 4H). GC/MS: m/z 311 (M⁺ + 2, 91), 309 (M⁺, 93), 203 (54), 188 (43), 174 (93), 132 (100), 117 (51), 104 (42).

***N*-Benzyl-6-bromohexanamide (37a)**. Eluted with CHCl₃; 81% yield. ¹H NMR (CDCl₃): δ 1.42–1.53 (m, 2H), 1.64–1.74 (m, 2H), 1.82–1.92 (m, 2H), 2.25 (app. t, 2H), 3.40 (t, 2H, $J = 6.8$ Hz), 4.44 (d, 2H, $J = 5.8$ Hz), 5.76 (br t, 1H, D₂O exchanged), 7.23–7.37 (m, 5H). GC/MS: m/z 285 (M⁺ + 2, 28), 283 (M⁺, 28), 149 (99), 106 (54), 91 (100).

6-Bromo-*N*-(4-pyridinylmethyl)hexanamide (37b). Eluted with CHCl₃/MeOH 19:1; 84% yield. ¹H NMR (CDCl₃): δ 1.34–1.43 (m, 2H), 1.53–1.61 (m, 2H), 1.72–1.80 (m, 2H), 2.17 (app. t, 2H), 3.30 (t, 2H, $J = 6.8$ Hz), 4.30 (d, 2H, $J = 5.8$ Hz), 5.76 (br t, 1H, D₂O exchanged), 7.09–7.11 (m, 2H), 8.40–8.42 (m, 2H). GC/MS: m/z 286 (M⁺ + 2, 2), 284 (M⁺, 3), 150 (100), 92 (58).

6-Bromo-*N*-(4-cyanophenylmethyl)hexanamide (37c). Eluted with CHCl₃/AcOEt 1:1; 78% yield. ¹H NMR (CDCl₃): δ 1.43–1.53 (m, 2H), 1.65–1.73 (m, 2H), 1.83–1.92 (m, 2H), 2.26 (app. t, 2H), 3.41 (t, 2H, $J = 6.6$ Hz), 4.49 (d, 2H, $J = 6.05$ Hz), 5.93 (br t, 1H, D₂O exchanged), 7.37 (d, 2H, $J = 8.5$ Hz), 7.59–7.63 (m, 2H). GC/MS: m/z 310 (M⁺ + 2, 13), 308 (M⁺, 13), 174 (100), 131 (27), 116 (82).

6-Bromo-*N*-(4-methanesulfonyloxyphenylmethyl)hexanamide (37d). Eluted with CHCl₃/AcOEt 1:1; 30% yield. ¹H NMR (CDCl₃): δ 1.43–1.53 (m, 2H), 1.62–1.75 (m, 2H), 1.83–1.92 (m, 2H), 2.24 (t, 2H, $J = 7.4$ Hz), 3.14 (s, 3H), 3.40 (t, 2H, $J = 6.6$ Hz), 4.44 (d, 2H, $J = 5.8$ Hz), 5.82 (br t, 1H, D₂O exchanged), 7.22–7.26 (m, 2H), 7.31–7.35 (m, 2H).

General Procedure for Preparation of Final Compounds 8–31.

A stirred mixture of alkylating agent **33a,b** and **37a–d** (8.0 mmol), 1-substituted piperazine (9.6 mmol), and K₂CO₃ (8.0 mmol) in acetonitrile was refluxed overnight. After cooling, the mixture was evaporated to dryness and H₂O (20 mL) was added to the residue. The aqueous phase was extracted with AcOEt (2 \times 30 mL). The collected organic layers were dried over Na₂SO₄ and evaporated under reduced pressure. The crude residue was chromatographed (CHCl₃/MeOH, 19:1, as eluent) to afford pure compounds **8–31**.

2-[6-[4-(2-methylthiophenyl)-1-piperazinyl]-1-oxohexyl]isoindoline (8). Yield 73%. ¹H NMR (CDCl₃): δ 1.39–1.48 (m, 2H), 1.57–1.68 (m, 2H), 1.77 (quintet, 2H, $J = 7.7$ Hz), 2.37–2.40 (m, 2H), 2.40 (s, 3H), 2.47 (app. t, 2H), 2.68 (br s, 4H), 3.06 (br s, 4H), 4.81 (s, 4H), 7.05–7.11 (m, 4H), 7.26–7.31 (m, 4H). GC/MS: m/z 424 (M⁺ + 1, 3), 423 (M⁺, 15), 245 (94), 221 (100), 136 (33). The hydrochloride salt melted at 187–189 °C (from MeOH/Et₂O). Anal. (C₂₅H₃₃N₃OS \cdot HCl \cdot 0.3H₂O) C, H, N.

2-[6-[4-(2-diphenyl)-1-piperazinyl]-1-oxohexyl]isoindoline (9). Yield 82%. ¹H NMR (CDCl₃): δ 1.33–1.43 (m, 2H), 1.49–1.59 (m, 2H), 1.72 (quintet, 2H, $J = 7.4$ Hz), 2.32–2.39 (m, 8H), 2.88 (app t, 4H), 4.79 (s, 4H), 7.02–7.09 (m, 2H), 7.23–7.30 (m, 7H), 7.36–7.41 (m, 2H), 7.61–7.64 (m, 2H). GC/MS: m/z 454 (M⁺ + 1, 5), 453 (M⁺, 7), 251 (71), 245 (100), 180 (48), 118 (30); mp 134–136 °C (from CHCl₃/*n*-hexane). Anal. (C₃₀H₃₅N₃O) C, H, N.

2-[6-[4-(2-(1-methylethyl)phenyl)-1-piperazinyl]-1-oxohexyl]isoindoline (10). Yield 56%. ¹H NMR (CDCl₃): δ 1.18 (s, 3H), 1.21 (s, 3H), 1.42–1.49 (m, 2H), 1.61–1.67 (m, 2H), 1.77 (quintet, 2H, $J = 7.4$ Hz), 2.40 (t, 2H, $J = 7.4$ Hz), 2.48 (app. t, 2H), 2.66 (br s, 4H), 2.93 (app t, 4H), 3.45–3.51 (m, 1H), 4.81 (s, 4H), 7.08–7.16 (m, 3H), 7.25–7.31 (m, 5H). GC/MS: m/z 420 (M⁺ + 1, 3), 419 (M⁺, 7), 245 (100), 217 (45), 118 (28); mp 114–116 °C (from CHCl₃/*n*-hexane). Anal. (C₂₇H₃₇N₃O) C, H, N.

2-[6-[4-(2-methoxyphenyl)-1-piperazinyl]-1-oxohexyl]isoindoline (11). Yield 74%. ¹H NMR (CDCl₃): δ 1.37–1.47 (m, 2H), 1.55–1.65 (m, 2H), 1.76 (quintet, 2H, $J = 7.4$ Hz), 2.39 (t, 2H, $J = 7.4$ Hz), 2.42–2.46 (m, 2H), 2.66 (br s, 4H), 3.10 (br s, 4H), 3.86 (s, 3H), 4.80 (s, 4H), 6.84–7.02 (m, 4H), 7.25–7.33 (m, 4H). GC/MS: m/z 408 (M⁺ + 1, 5), 407 (M⁺, 18), 392 (39), 245 (74), 205 (100), 118 (50). The hydrochloride salt melted at 198–200 °C (from MeOH/Et₂O). Anal. (C₂₅H₃₃N₃O₂ \cdot 2HCl \cdot 0.2H₂O) C, H, N.

2-[6-[4-(2-methylthiophenyl)-1-piperazinyl]-1-oxohexyl]-1,2,3,4-tetrahydroisoquinoline (12). Yield 60%. ¹H NMR (CDCl₃): δ 1.38–1.46 (m, 2H), 1.58–1.61 (m, 2H), 1.66–1.76 (m, 2H), 2.41 (s, 3H), 2.42–2.47 (m, 4H), 2.64 (br s, 4H), 2.85 (app t, 1H), 2.90 (t, 1H, $J = 5.8$ Hz), 3.06 (br s, 4H), 3.68 (app t, 1H), 3.83 (t, 1H, $J = 6.05$ Hz), 4.62 (s, 1H), 4.73 (s, 1H), 7.04–7.10 (m, 4H),

7.12–7.22 (m, 4H). GC/MS: *m/z* 438 ($M^+ + 1$, 4), 437 (M^+ , 8), 259 (83), 221 (100), 206 (30), 132 (54). The hydrochloride salt melted at 112–114 °C dec (from MeOH/Et₂O). Anal. (C₂₆H₃₅N₃O₂·HCl·H₂O) C, H, N.

2-[6-[4-(2-Diphenyl)-1-piperazinyl]-1-oxohexyl]-1,2,3,4-tetrahydroisoquinoline (13). Yield 48%. ¹H NMR (CDCl₃): δ 1.30–1.43 (m, 2H), 1.47–1.52 (m, 2H), 1.61–1.73 (m, 2H), 2.36–2.42 (m, 8H), 2.82–2.88 (m, 6H), 3.66 (app t, 1H), 3.82 (app t, 1H), 4.60 (s, 1H), 4.72 (s, 1H), 7.02–7.10 (m, 2H), 7.12–7.31 (m, 7H), 7.36–7.41 (m, 2H), 7.61–7.64 (m, 2H). GC/MS: *m/z* 468 ($M^+ + 1$, 4), 467 (M^+ , 10), 259 (100), 251 (78), 180 (65). The hydrochloride salt melted at 70–72 °C dec (from MeOH/Et₂O). Anal. (C₃₁H₃₇N₃O·HCl·H₂O) C, H, N.

2-[6-[4-(2-(1-Methylethyl)phenyl)-1-piperazinyl]-1-oxohexyl]-1,2,3,4-tetrahydroisoquinoline (14). Yield 95%. ¹H NMR (CDCl₃): δ 1.19 (s, 3H), 1.21 (s, 3H), 1.38–1.46 (m, 2H), 1.55–1.62 (m, 2H), 1.66–1.77 (m, 2H), 2.40–2.47 (m, 4H), 2.67 (br s, 4H), 2.85 (app t, 1H), 2.88–2.94 (m, 5H), 3.44–3.53 (m, 1H), 3.67 (app t, 1H), 3.83 (t, 1H, *J* = 6.05 Hz), 4.62 (s, 1H), 4.73 (s, 1H), 7.06–7.20 (m, 6H), 7.21–7.26 (m, 2H). GC/MS: *m/z* 434 ($M^+ + 1$, 2), 433 (M^+ , 5), 259 (100), 217 (38). The oxalate salt melted at 210–212 °C (from MeOH/Et₂O). Anal. (C₂₈H₃₉N₃O·(COOH)₂) C, H, N.

2-[6-[4-(2-Methoxyphenyl)-1-piperazinyl]-1-oxohexyl]-1,2,3,4-tetrahydroisoquinoline (15). Yield 90%. ¹H NMR (CDCl₃): δ 1.35–1.45 (m, 2H), 1.55–1.61 (m, 2H), 1.65–1.77 (m, 2H), 2.39–2.46 (m, 4H), 2.67 (br s, 4H), 2.85 (t, 1H, *J* = 6.05 Hz), 2.90 (app t, 1H), 3.11 (br s, 4H), 3.68 (app t, 1H), 3.83 (t, 1H, *J* = 6.05 Hz), 3.86 (s, 3H), 4.62 (s, 1H), 4.73 (s, 1H), 6.84–7.03 (m, 4H), 7.10–7.22 (m, 4H). GC/MS: *m/z* 422 ($M^+ + 1$, 5), 421 (M^+ , 16), 406 (46), 259 (83), 205 (100), 190 (32). The hydrochloride salt melted at 164–166 °C (from MeOH/Et₂O). Anal. (C₂₆H₃₅N₃O₂·2HCl·0.7H₂O) C, H, N.

***N*-Benzyl-4-(2-methylthiophenyl)-1-piperazinehexanamide (16).** Yield 90%. ¹H NMR (CDCl₃): δ 1.34–1.42 (m, 2H), 1.52–1.62 (m, 2H), 1.71 (quintet, 2H, *J* = 7.4 Hz), 2.23 (t, 2H, *J* = 7.4 Hz), 2.41 (s, 3H), 2.42–2.45 (m, 2H), 2.64 (br s, 4H), 3.03 (br t, 4H), 4.44 (d, 2H, *J* = 5.5 Hz), 5.80 (br t, 1H, D₂O exchanged), 7.04–7.11 (m, 4H), 7.26–7.36 (m, 5H). GC/MS: *m/z* 442 ($M^+ + 1$, 3), 441 (M^+ , 10), 251 (100), 233 (38), 180 (61). The hydrochloride salt melted at 150–152 °C (from MeOH/Et₂O). Anal. (C₂₄H₃₃N₃O₂·HCl·H₂O) C, H, N.

***N*-Benzyl-4-(2-diphenyl)-1-piperazinehexanamide (17).** Yield 90%. ¹H NMR (CDCl₃): δ 1.27–1.37 (m, 2H), 1.44–1.54 (m, 2H), 1.66 (quintet, 2H, *J* = 7.4 Hz), 2.20 (t, 2H, *J* = 7.4 Hz), 2.30 (app t, 2H), 2.35 (br s, 4H), 2.85 (app t, 4H), 4.43 (d, 2H, *J* = 5.8 Hz), 5.79 (br t, 1H, D₂O exchanged), 7.02–7.09 (m, 2H), 7.23–7.41 (m, 10H), 7.61–7.64 (m, 2H). GC/MS: *m/z* 412 ($M^+ + 1$, 3), 411 (M^+ , 6), 233 (42), 221 (100), 206 (27). The hydrochloride salt melted at 212–214 °C (from MeOH/Et₂O). Anal. (C₂₉H₃₅N₃O·HCl) C, H, N.

***N*-Benzyl-4-[2-(1-methylethyl)phenyl]-1-piperazinehexanamide (18).** Yield 90%. ¹H NMR (CDCl₃): δ 1.19 (s, 3H), 1.21 (s, 3H), 1.33–1.43 (m, 2H), 1.53–1.63 (m, 2H), 1.71 (quintet, 2H, *J* = 7.4 Hz), 2.24 (app t, 2H), 2.43 (app t, 2H), 2.62 (br s, 4H), 2.92 (app t, 4H), 3.41–3.55 (m, 1H), 4.45 (d, 2H, *J* = 5.8 Hz), 5.80 (br t, 1H, D₂O exchanged), 7.06–7.18 (m, 4H), 7.24–7.37 (m, 5H). GC/MS: *m/z* 408 ($M^+ + 1$, 2), 407 (M^+ , 4), 233 (100), 217 (73), 160 (21). The hydrochloride salt melted at 116–119 °C (from MeOH/Et₂O). Anal. (C₂₆H₃₇N₃O·HCl·1.2H₂O) C, H, N.

***N*-Benzyl-4-(2-methoxyphenyl)-1-piperazinehexanamide (19).** Yield 82%. ¹H NMR (CDCl₃): δ 1.32–1.42 (m, 2H), 1.52–1.62 (m, 2H), 1.71 (quintet, 2H, *J* = 7.4 Hz), 2.23 (t, 2H, *J* = 7.4 Hz), 2.42 (app t, 2H), 2.66 (br s, 4H), 3.10 (br s, 4H), 3.86 (s, 3H), 4.44 (d, 2H, *J* = 5.5 Hz), 5.79 (br t, 1H, D₂O exchanged), 6.84–7.03 (m, 4H), 7.27–7.37 (m, 5H). GC/MS: *m/z* 396 ($M^+ + 1$, 4), 395 (M^+ , 15), 233 (27), 205 (100), 190 (29). The hydrochloride salt melted at 174–176 °C (from MeOH/Et₂O). Anal. (C₂₄H₃₃N₃O₂·2HCl·0.5H₂O) C, H, N.

4-(2-Methylthiophenyl)-*N*-(4-pyridinylmethyl)-1-piperazinehexanamide (20). Yield 87%. ¹H NMR (CDCl₃): δ 1.36–1.46 (m, 2H), 1.61–1.69 (m, 2H), 1.71–1.79 (m, 2H), 2.31 (t, 2H, *J* = 7.4 Hz),

2.40 (s, 3H), 2.53 (app t, 2H), 2.75 (br s, 4H), 3.10 (br t, 4H), 4.46 (d, 2H, *J* = 6.1 Hz), 6.23 (br t, 1H, D₂O exchanged), 7.03–7.12 (m, 4H), 7.20 (dd, 2H, *J* = 1.65, 4.4 Hz), 8.55 (dd, 2H, *J* = 1.65, 4.4 Hz). GC/MS: *m/z* 413 ($M^+ + 1$, 3), 412 (M^+ , 16), 397 (39), 234 (72), 221 (100), 206 (59); mp 50–52 °C (from *n*-hexane). Anal. (C₂₃H₃₂N₄O₂) C, H, N.

4-(2-Diphenyl)-*N*-(4-pyridinylmethyl)-1-piperazinehexanamide (21). Yield 64%. ¹H NMR (CDCl₃): δ 1.28–1.38 (m, 2H), 1.43–1.54 (m, 2H), 1.68 (q, 2H, *J* = 7.4 Hz), 2.25 (t, 2H, *J* = 7.4 Hz), 2.31–2.33 (m, 2H), 2.35 (br s, 4H), 2.86 (app t, 4H), 4.44 (d, 2H, *J* = 6.1 Hz), 6.00 (br t, 1H, D₂O exchanged), 7.01–7.09 (m, 2H), 7.16–7.18 (m, 2H), 7.22–7.31 (m, 3H), 7.36–7.41 (m, 2H), 7.60–7.64 (m, 2H), 8.54 (dd, 2H, *J* = 1.7, 4.4 Hz). GC/MS: *m/z* 443 ($M^+ + 1$, 1), 442 (M^+ , 10), 251 (82), 234 (78), 180 (100). The hydrochloride salt melted at 50 °C dec (from MeOH/Et₂O). Anal. (C₂₈H₃₄N₄O·2HCl·1.5H₂O) C, H, N.

4-[2-(1-Methylethyl)phenyl]-*N*-(4-pyridinylmethyl)-1-piperazinehexanamide (22). Yield 95%. ¹H NMR (CDCl₃): δ 1.18 (s, 3H), 1.21 (s, 3H), 1.35–1.45 (m, 2H), 1.55–1.65 (m, 2H), 1.73 (quintet, 2H, *J* = 7.4 Hz), 2.29 (t, 2H, *J* = 7.4 Hz), 2.44 (app t, 2H), 2.64 (br s, 4H), 2.94 (app t, 4H), 3.43–3.52 (m, 1H), 4.46 (d, 2H, *J* = 6.1 Hz), 6.10 (br t, 1H, D₂O exchanged), 7.06–7.16 (m, 4H), 7.18–7.20 (m, 1H), 7.24–7.25 (m, 1H), 8.55 (dd, 2H, *J* = 1.4, 4.4 Hz). GC/MS: *m/z* 409 ($M^+ + 1$, 1), 408 (M^+ , 6), 234 (100), 217 (58), 160 (30). The hydrochloride salt melted at 163–166 °C dec (from MeOH/Et₂O). Anal. (C₂₅H₃₆N₄O·3HCl·H₂O) C, H, N.

4-(2-Methoxyphenyl)-*N*-(4-pyridinylmethyl)-1-piperazinehexanamide (23). Yield 70%. ¹H NMR (CDCl₃): δ 1.34–1.43 (m, 2H), 1.53–1.63 (m, 2H), 1.67–1.77 (m, 2H), 2.28 (t, 2H, *J* = 7.4 Hz), 2.42 (app t, 2H), 2.66 (br s, 4H), 3.10 (br s, 4H), 3.85 (s, 3H), 4.45 (d, 2H, *J* = 6.1 Hz), 6.10 (br t, 1H, D₂O exchanged), 6.84–7.03 (m, 4H), 7.18 (dd, 2H, *J* = 1.6, 4.4 Hz), 8.54 (dd, 2H, *J* = 1.6, 4.4 Hz). GC/MS: *m/z* 397 ($M^+ + 1$, 2), 396 (M^+ , 10), 234 (36), 205 (100), 190 (38); mp 93–94 °C (from *n*-hexane). Anal. (C₂₃H₃₂N₄O₂) C, H, N.

***N*-(4-Cyanophenylmethyl)-4-(2-methylthiophenyl)-1-piperazinehexanamide (24).** Yield 66%. ¹H NMR (CDCl₃): δ 1.33–1.43 (m, 2H), 1.52–1.62 (m, 2H), 1.66–1.76 (m, 2H), 2.27 (t, 2H, *J* = 7.4 Hz), 2.40 (s, 3H), 2.42–2.45 (m, 2H), 2.63 (br s, 4H), 3.03 (app t, 4H), 4.50 (d, 2H, *J* = 4.5 Hz), 6.00 (br t, 1H, D₂O exchanged), 7.02–7.13 (m, 4H), 7.36–7.39 (m, 2H), 7.60–7.63 (m, 2H). GC/MS: *m/z* 437 ($M^+ + 1$, 5), 436 (M^+ , 16), 221 (100), 206 (19), 116 (23). The hydrochloride salt melted at 100–103 °C dec (from MeOH/Et₂O). Anal. (C₂₅H₃₃N₄O₂·HCl·H₂O) C, H, N.

***N*-(4-Cyanophenylmethyl)-4-(2-diphenyl)-1-piperazinehexanamide (25).** Yield 90%. ¹H NMR (CDCl₃): δ 1.27–1.37 (m, 2H), 1.44–1.54 (m, 2H), 1.66 (quintet, 2H, *J* = 7.4 Hz), 2.23 (t, 2H, *J* = 7.4 Hz), 2.28–2.32 (m, 2H), 2.35 (br s, 4H), 2.85 (app t, 4H), 4.48 (d, 2H, *J* = 6.1 Hz), 5.97 (br t, 1H, D₂O exchanged), 7.00–7.10 (m, 2H), 7.22–7.31 (m, 3H), 7.33–7.41 (m, 4H), 7.58–7.64 (m, 4H). GC/MS: *m/z* 467 ($M^+ + 1$, 9), 466 (M^+ , 20), 251 (100), 180 (51), 116 (26); mp 50 °C dec (from *n*-hexane). Anal. (C₃₀H₃₄N₄O) C, H, N.

***N*-(4-Cyanophenylmethyl)-4-[2-(1-methylethyl)phenyl]-1-piperazinehexanamide (26).** Yield 83%. ¹H NMR (CDCl₃): δ 1.18 (s, 3H), 1.21 (s, 3H), 1.34–1.43 (m, 2H), 1.53–1.64 (m, 2H), 1.72 (quintet, 2H, *J* = 7.4 Hz), 2.28 (t, 2H, *J* = 7.4 Hz), 2.43 (app t, 2H), 2.62 (br s, 4H), 2.92 (app t, 4H), 3.43–3.52 (m, 1H), 4.50 (d, 2H, *J* = 6.1 Hz), 6.03 (br t, 1H, D₂O exchanged), 7.07–7.18 (m, 3H), 7.24–7.27 (m, 1H), 7.38 (d, 2H, *J* = 8.3 Hz), 7.60–7.63 (m, 2H). GC/MS: *m/z* 433 ($M^+ + 1$, 3), 432 (M^+ , 8), 258 (100), 217 (99), 160 (34), 132 (31). The hydrochloride salt melted at 83–85 °C dec (from MeOH/Et₂O). Anal. (C₂₇H₃₆N₄O·2HCl) C, H, N.

***N*-(4-Cyanophenylmethyl)-4-(2-methoxyphenyl)-1-piperazinehexanamide (27).** Yield 95%. ¹H NMR (CDCl₃): δ 1.33–1.43 (m, 2H), 1.53–1.63 (m, 2H), 1.71 (quintet, 2H, *J* = 7.4 Hz), 2.27 (t, 2H, *J* = 7.4 Hz), 2.43 (app t, 2H), 2.67 (br s, 4H), 3.10 (app t, 4H), 3.86 (s, 3H), 4.49 (d, 2H, *J* = 6.1 Hz), 6.03 (br t, 1H, D₂O exchanged), 6.84–6.89 (m, 1H), 6.916.96 (m, 2H), 6.97–7.03 (m, 1H), 7.37 (d, 2H, *J* = 8.5 Hz), 7.59–7.62 (m, 2H). GC/MS: *m/z*

421 ($M^+ + 1$, 7), 420 (M^+ , 24), 205 (100), 190 (20); mp 123–125 °C dec (from $CHCl_3/n$ -hexane). Anal. ($C_{25}H_{32}N_4O_2$) C, H, N.

N-(4-Methanesulfonyloxyphenylmethyl)-4-(2-methylthiophenyl)-1-piperazinehexanamide (28). Yield 95%. 1H NMR ($CDCl_3$): δ 1.32–1.42 (m, 2H), 1.53–1.63 (m, 2H), 1.70 (quintet, 2H, $J = 7.4$ Hz), 2.24 (t, 2H, $J = 7.4$ Hz), 2.41 (s, 3H), 2.43–2.46 (m, 2H), 2.65 (br s, 4H), 3.04 (app t, 4H), 3.13 (s, 3H), 4.45 (d, 2H, $J = 5.8$ Hz), 5.94 (br t, 1H, D_2O exchanged), 7.03–7.16 (m, 4H), 7.23–7.25 (m, 2H), 7.32–7.35 (m, 2H). ESI^+/MS m/z 506 (MH $^+$). $ESI^+/MS/MS$ m/z 341 (42), 298 (100), 249 (49), 185 (53). The hydrochloride salt melted at 118–120 °C (from MeOH/ Et_2O). Anal. ($C_{25}H_{35}N_3O_4S_2 \cdot HCl \cdot 0.7H_2O$) C, H, N.

N-(4-Methanesulfonyloxyphenylmethyl)-4-(2-diphenyl)-1-piperazinehexanamide (29). Yield 95%. 1H NMR ($CDCl_3$): δ 1.27–1.36 (m, 2H), 1.44–1.54 (m, 2H), 1.66 (quintet, 2H, $J = 7.7$ Hz), 2.21 (t, 2H, $J = 7.7$ Hz), 2.28–2.33 (m, 2H), 2.36 (br s, 4H), 2.86 (app t, 4H), 3.13 (s, 3H), 4.43 (d, 2H, $J = 6.1$ Hz), 5.89 (br t, 1H, D_2O exchanged), 7.01–7.10 (m, 2H), 7.22–7.41 (m, 9H), 7.61–7.64 (m, 2H). ESI^+/MS m/z 536 (MH $^+$). $ESI^+/MS/MS$ m/z 298 (100), 251 (32), 185 (56). The hydrochloride salt melted at 160–163 °C (from MeOH/ Et_2O). Anal. ($C_{30}H_{39}N_3O_4S \cdot HCl \cdot H_2O$) C, H, N.

N-(4-Methanesulfonyloxyphenylmethyl)-4-[2-(1-methylethyl)phenyl]-1-piperazinehexanamide (30). Yield 88%. 1H NMR ($CDCl_3$): δ 1.18 (s, 3H), 1.21 (s, 3H), 1.33–1.43 (m, 2H), 1.53–1.63 (m, 2H), 1.71 (quintet, 2H, $J = 7.7$ Hz), 2.25 (t, 2H, $J = 7.7$ Hz), 2.42 (app. t, 2H), 2.61 (br s, 4H), 2.92 (app t, 4H), 3.13 (s, 3H), 3.43–3.53 (m, 1H), 4.45 (d, 2H, $J = 4.5$ Hz), 5.94 (br t, 1H, D_2O exchanged), 7.06–7.18 (m, 4H), 7.22–7.26 (m, 2H), 7.32–7.35 (m, 2H). ESI^+/MS m/z 502 (MH $^+$). $ESI^+/MS/MS$ m/z 298 (100), 185 (56). The hydrochloride salt melted at 83–85 °C dec (from MeOH/ Et_2O). Anal. ($C_{27}H_{39}N_3O_4S \cdot HCl \cdot 1.5H_2O$) C, H, N.

N-(4-Methanesulfonyloxyphenylmethyl)-4-(2-methoxyphenyl)-1-piperazinehexanamide (31). Yield 80%. 1H NMR ($CDCl_3$): δ 1.32–1.42 (m, 2H), 1.52–1.62 (m, 2H), 1.70 (quintet, 2H, $J = 7.4$ Hz), 2.24 (t, 2H, $J = 7.4$ Hz), 2.40 (app. t, 2H), 2.65 (br s, 4H), 3.09 (br s, 4H), 3.13 (s, 3H), 3.86 (s, 3H), 4.44 (d, 2H, $J = 6.1$ Hz), 5.89 (br t, 1H, D_2O exchanged), 6.84–7.03 (m, 4H), 7.21–7.27 (m, 2H), 7.31–7.36 (m, 2H). ESI^+/MS m/z 490 (MH $^+$). $ESI^+/MS/MS$ m/z 396 (65), 298 (100), 185 (56). The hydrochloride salt melted at 146–149 °C dec (from MeOH/ Et_2O). Anal. ($C_{25}H_{35}N_3O_5S \cdot 2HCl \cdot H_2O$) C, H, N.

Lipophilicity. Lipophilicity indices were measured by a reversed-phase HPLC method consisting in a Perkin-Elmer series 200 LC apparatus equipped with a Perkin-Elmer 785A UV/vis detector set at 254 nm. UV signals were monitored and obtained peaks integrated using a personal computer running Perkin-Elmer Turbochrom Software. The capacity factors were measured with a Phenomenex Prodigy ODS-3 RP-18 (250 mm \times 4.6 mm, 5 μ m particle size) as nonpolar stationary phase and with MeOH/0.01 M phosphate buffer pH 6 (70:30 v/v) as mobile phase. This ratio was found to be the best compromise for a large number of derivatives. All compounds were dissolved in methanol, and the measurements were made at a flow rate of 1 mL/min. Capacity factors were calculated as: $k' = (t_R - t_0)/t_0$, where t_R is the retention time of the solute and t_0 is the column dead time, measured as the solvent front.

Biological Methods. 1. General. Male albino Dunkin–Hartley guinea pigs (300–350 g) were from Harlan (S. Pietro al Natisone, Italy). The animals were handled according to internationally accepted principles for care of laboratory animals (EEC Council Directive 86/609, O. J. no. L358, Dec 18, 1986). Rat recombinant serotonin 5-HT $_7$ receptors and human recombinant serotonin 5-HT $_{1A}$ receptors expressed in HEK-293 cells were purchased from Perkin-Elmer (Zaventem, Belgium). Human recombinant D $_{2L}$ dopamine receptors expressed in rat C6 glioma cells were gifted by Prof. Roberto Maggio (Università di L'Aquila, Italy). [3H]-LSD, [3H]-8-OH-DPAT, and [3H]-spiroperidol were obtained from Perkin-Elmer-NEN (Zaventem, Belgium). Compound **2**, 5-CT, and substance P were purchased from Tocris Bioscience (Bristol, UK). 8-OH-DPAT hydrobromide was from RBI. Haloperidol were purchased from Sigma-Aldrich (Milan, Italy).

2. Radioligand Binding Assay at Rat Cloned 5-HT $_7$ Rs. Binding of [3H]-LSD at rat cloned 5-HT $_7$ receptor was performed according to Jasper et al.⁴³ with minor modifications. In 1 mL of incubation buffer (50 mM Tris, 10 mM MgCl $_2$ and 0.5 mM EDTA, pH 7.4) were suspended 30 μ g of membranes, 2.5 nM [3H]-LSD, the drugs, or reference compound (6–9 concentrations). The samples were incubated for 60 min at 37 °C. The incubation was stopped by rapid filtration on GF/A glass fiber filters (presoaked in 0.5% polyethylenimine for 30 min). The filters were washed with 3 \times 53 mL of ice-cold buffer (50 mM Tris, pH 7.4). Nonspecific binding was determined in the presence of 10 μ M 5-CT. Approximately 90% of specific binding was determined under these conditions.

3. Radioligand Binding Assay at Human Cloned 5-HT $_{1A}$ Receptor. Human 5-HT $_{1A}$ serotonin receptors stably expressed in HEK-293 cells were radiolabeled with 1.0 nM [3H]-8-OH-DPAT.⁴⁴ Samples containing 40 μ g of membrane protein and different concentrations of each compound ranging from 0.1 nM to 10 μ M were incubated in a final volume of 500 μ L of 50 mM Tris-HCl pH 7.4, 5 mM MgSO $_4$ for 120 min at 37 °C. After this incubation time, samples were filtered through GF/C presoaked in polyethylenimine 0.5% for at least 30 min prior to use. The filters were washed twice with 1 mL of ice-cold buffer (50 mM Tris-HCl, pH 7.4). Nonspecific binding was determined in the presence of 10 μ M 5-HT.

4. Radioligand Binding Assay at Human Cloned D $_{2L}$ Dopaminergic Receptors. Binding of [3H]-spiroperidol at human cloned receptors was performed according to Scarselli et al.⁴⁵ with minor modifications. The incubation buffer (120 mM NaCl, 5.0 mM KCl, 5.0 mM MgCl $_2$, 1 mM EDTA, 50 mM Tris, pH 7.4) contained 100 μ g of dopamine dilute membranes, 0.30–0.50 nM [3H]-spiroperidol ($K_d = 0.093$ nM), and 6–9 concentrations of drug solution in a final volume of 500 μ L. The samples were incubated for 120 min at 25 °C, then the incubation was stopped by rapid filtration through Whatman GF/C glass fiber filters (presoaked in 0.5% polyethylenimine for 60 min). The filters were washed 3 \times 1 mL of ice-cold 50 mM Tris, 0.9% NaCl, pH 7.4. Non specific binding was determined in the presence of 10 μ M haloperidol. The radioactivity bound to the filters was measured by liquid scintillation using LS6500 multipurpose scintillation Counter, Beckman.

5. Isolated Guinea-Pig Ileum Assay. guinea pigs were anesthetized and then decapitated and the proximal ileum removed. The intestine was carefully flushed several times with warm Krebs–Henseleit solution (118 mM NaCl, 25 mM NaHCO $_3$, 4.7 mM KCl, 0.6 mM MgSO $_4$, 1.2 mM KH $_2$ PO $_4$, 1.2 mM CaCl $_2$, 11.2 mM glucose, pH 7.4). Whole ileal segments, of about 3 cm in length, were suspended under 1.0 g tension in Krebs solution gassed with 95% O $_2$ and 5% CO $_2$ and maintained at 37 °C. According to Carter et al.⁴⁶ with minor modification, the bathing medium contained 1 μ M atropine to antagonize cholinergically mediated contractions due to activation of 5-HT $_3$ and 5-HT $_4$ receptors, 1 μ M ketanserin to block 5-HT $_{2A}$ receptors, and 1 μ M pyrilamine to block H $_1$ receptors. Changes in tension of the tissue were recorded by Fort 10 Original WPI isometric transducer (2Biological Instruments, Italy) connected to a PowerLab/400 workstation.⁴⁷ Tissue responses were recorded as gram changes in isometric tension and expressed as percentage of reduction in the height of the contraction. Tissue was contracted by 100 nM substance P. This value was preliminary determined by concentration–response curves (1 nM to 200 nM). 100 nM substance P elicited 80% of maximum contraction. The reference agonist 5-CT was added 5 min before substance P addition and noncumulative concentration–response curves were constructed (0.001– μ M). We have determined that 5-CT induced relaxation with maximal response (39%) at 3 μ M concentration. Analogously, each compound tested (0.001–10 μ M) was added 5 min before substance P addition and noncumulative concentration–response curve was constructed. Relaxant responses to full agonists 5-CT **13**, **21**, and **25** were surmountably antagonized by **2** (0.1–3 μ M). The isolated guinea pig ileum was equilibrated for 15 min with **2** before constructing concentration–response curves of tested compounds. The corresponding pA $_2$ values of **2** versus each studied

agonist are listed in Table 4. Desensitization was then used to discriminate if the studied compounds were acting as 5-HT₇ receptor agonists or nonspecific smooth muscle relaxant. The agonist studies were consequently repeated in the presence of 3 μ M 5-CT, following equilibration with 5-CT for 60 min, during which time the bathing solution was changed at 15 min intervals. This concentration of 5-CT abolished relaxant responses emanating from 5-HT₇ receptor stimulation.

6. Disposition Studies. Male CD1 albino mice, 25–30 g (Charles River, Italy) were used. Procedures involving animals and their care were conducted in conformity with the institutional guidelines that are in compliance with national (D.L., no. 116, G.U., suppl. 40, 18 Febbraio 1992, Circolare no. 8, G.U., 14 Luglio 1994) and international laws and policies (EEC Council Directive 86/609, O. J. L358, 1, Dec 12, 1987; Guide for the Care and Use of Laboratory, U.S. National Research Council, 1996).

Mice were given the test compounds intraperitoneally (10 mg/kg) and were killed by decapitation at various times thereafter. Mixed arteriovenous trunk blood was collected in heparinized tubes, centrifuged at 3000g for 10 min, and the plasma was stored at –20 °C. Brain was removed immediately, blotted with paper to remove surface blood, and quickly frozen in dry ice. Compounds and their 1-arylpiperazine metabolites were extracted from plasma and brain homogenate and quantified by reversed-phase HPLC with UV detection (230 nm). Briefly: to 0.1 mL of plasma, 0.2 mL of 20 mM of ammonium bicarbonate and 0.02 mL of a methanolic solution of the internal standard (100 μ g/mL) were added; samples were then extracted twice with 1.5 mL of hexane containing 1% of isoamyl alcohol, and the combined extracts were evaporated to dryness and reconstituted in 0.15 mL of the mobile phase, which was injected into the chromatographic column. Brain tissue was homogenized in distilled water (1 g/10 mL), and 1 mL of the homogenate was extracted twice with 1.5 mL of hexane/isoamyl alcohol as described for plasma. Then, the organic phase was shaken with 0.2 mL of the mobile phase (compound **25** only); after centrifugation, 0.1 mL of the aqueous phase was injected into the chromatographic column.

Separation was done on a Brownlee Laboratory Spheri 5 RP 8 (4.6 mm \times 250 mm; 5 μ m), with 0.01 M KH₂PO₄/CH₃CN/CH₃OH (50:45:5 v/v, compound **25**; 50:40:10 v/v, compound **4**), at pH 3.5, as the mobile phase. A derivative of the present series was used as internal standard.

Standard curves were prepared by spiking blank mouse plasma and brain homogenate. The lower limit for quantification was about 0.1 μ g/mL in plasma and 0.1 μ g/g in brain tissue, using respectively 0.1 mL of plasma and 1 mL of brain homogenate (or approximately 100 mg of brain tissue). At these concentrations the coefficient of variation for the precision of the assay was 10–20%. Higher concentrations generally gave coefficients of variation less than 10%, regardless of the compound and tissue analyzed. Brain concentrations were not corrected for compounds **4** and **25** contributed by the residual blood, because this generally amounted to only 1–3% of the measured brain concentrations, assuming a mean value of 20 μ L per gram of brain.⁴⁸

7. Statistical and Pharmacokinetic Analysis. The inhibition curves on the different binding sites of the compounds reported in Tables 2 and 3 were analyzed by nonlinear curve fitting utilizing the GraphPad Prism program.⁴⁹ The value for the inhibition constant, K_i , was calculated by using the Cheng–Prusoff equation.⁵⁰ Agonist potencies, expressed as EC₅₀, were obtained from nonlinear iterative curve fitting by GraphPad Prism.

Mean plasma and brain and plasma area under the concentration–time curve (AUC_t) were determined using the linear trapezoidal rule and extrapolated to infinity (AUC), when possible, using the elimination rate constant. The maximum concentration (C_{max}) and the time of its occurrence were read directly from the plasma and brain concentration–time data. Standard noncompartmental analysis, using the Win Nonlin software Pro Node 4.1 (Pharsight Co, Mountain View, CA) was done to calculate total body clearance, volume of distribution, and elimination half-life ($t_{1/2}$).

Supporting Information Available: Elemental analysis data of target compounds. This material is available free of charge via the Internet at <http://pubs.acs.org>.

References

- (1) Hoyer, D.; Hannon, J. P.; Martin, G. R. Molecular, pharmacological and functional diversity of 5-HT receptors. *Pharmacol. Biochem. Behav.* **2002**, *71*, 533–554.
- (2) Hedlund, P. B.; Sutcliffe, J. G. Functional, molecular and pharmacological advances in 5-HT₇ receptor research. *Trends Pharmacol. Sci.* **2004**, *25*, 481–486.
- (3) Bickmeyer, U.; Heine, M.; Manzke, T.; Richter, D. W. Differential modulation of Ih by 5-HT receptors in mouse CA1 hippocampal neurons. *Eur. J. Neurosci* **2002**, *16*, 209–218.
- (4) Belenky, M. A.; Pickard, G. E. Subcellular distribution of 5-HT_{1B} and 5-HT₇ receptors in the mouse suprachiasmatic nucleus. *J. Comp. Neurol.* **2001**, *432*, 371–388.
- (5) Neumaier, J. F.; Sexton, T. J.; Yracheta, J.; Diaz, A. M.; Brownfield, M. Localization of 5-HT₇ receptors in rat brain by immunocytochemistry, in situ hybridization, and agonist stimulated cFos expression. *J. Chem. Neuroanat.* **2001**, *21*, 63–73.
- (6) Muneoka, K. T.; Takigawa, M. 5-Hydroxytryptamine₇ (5-HT₇) receptor immunoreactivity-positive “stigmoid body”-like structure in developing rat brains. *Int. J. Dev. Neurosci* **2003**, *21*, 133–143.
- (7) Varnäs, K.; Thomas, D. R.; Tupala, E.; Tiitonen, J.; Hall, H. Distribution of 5-HT₇ receptors in the human brain: a preliminary autoradiographic study using [³H]SB-269970. *Neurosci. Lett.* **2004**, *367*, 313–316.
- (8) Mullins, U. L.; Gianutsos, G.; Eison, A. S. Effects of antidepressants on 5-HT₇ receptor regulation in the rat hypothalamus. *Neuropsychopharmacology* **1999**, *21*, 352–367.
- (9) Guscott, M.; Bristow, L. J.; Hadingham, K.; Rosahl, T. W.; Beer, M. S.; Stanton, J. A.; Bromidge, F.; Owens, A. P.; Huscroft, I.; Myers, J.; Rupniak, N. M.; Patel, S.; Whiting, P. J.; Hutson, P. H.; Fone, K. C.; Biello, S. M.; Kulagowski, J. J.; McAllister, G. Genetic knockout and pharmacological blockade studies of the 5-HT₇ receptor suggest therapeutic potential in depression. *Neuropharmacology* **2005**, *48*, 492–502.
- (10) Hedlund, P. B.; Huitron-Resendiz, S.; Henriksen, S. J.; Sutcliffe, J. G. 5-HT₇ Receptor inhibition and inactivation induce antidepressantlike behavior and sleep pattern. *Biol. Psychiatry* **2005**, *58*, 831–837.
- (11) Wesolowska, A.; Nikiforuk, A.; Stachowicz, K. Potential anxiolytic and antidepressant effects of the selective 5-HT₇ receptor antagonist SB-269970 after intrahippocampal administration to rats. *Eur. J. Pharmacol.* **2006**, *553*, 185–190.
- (12) Bonaventure, P.; Kelly, L.; Aluisio, L.; Shelton, J.; Lord, B.; Galici, R.; Miller, K.; Atak, J.; Lovenberg, T. W.; Dugovic, C. Selective blockade of 5-hydroxytryptamine 5-HT₇ receptors enhances 5-HT transmission, antidepressant-like behavior, and rapid eye movement sleep suppression induced by citalopram in rodents. *J. Pharmacol. Exp. Ther.* **2007**, *321*, 690–698.
- (13) Hedlund, P. B.; Sutcliffe, J. G. The 5-HT₇ receptor influences stereotypic behavior in a model of obsessive-compulsive disorder. *Neurosci. Lett.* **2007**, *414*, 247–251.
- (14) Pérez-García, G.; Gonzalez-Espinosa, C.; Meneses, A. An mRNA expression analysis of stimulation and blockade of 5-HT₇ receptors during memory consolidation. *Behav. Brain Res.* **2006**, *169*, 83–92.
- (15) Meneses, A. Effects of the 5-HT₇ receptor antagonists SB-269970 and DR4004 in autoshaping Pavlovian/instrumental learning task. *Behav. Brain Res.* **2004**, *155*, 275–282.
- (16) Gasbarri, A.; Cifariello, A.; Pompili, A.; Meneses, A. Effect of 5-HT₇ antagonist SB-269970 in the modulation of working and reference memory in the rat. *Behav. Brain Res.* **2008**, doi: 10.1016/j.bbr.2007.12.020.
- (17) Semenova, S.; Geyer, M. A.; Sutcliffe, J. G.; Markou, A.; Hedlund, P. B. Inactivation of the 5-HT₇ receptor partially blocks phencyclidine-induced disruption of prepulse inhibition. *Biol. Psychiatry* **2008**, *63*, 98–105.
- (18) Galici, R.; Boggs, J. D.; Miller, K. L.; Bonaventure, P.; Atack, J. R. Effects of SB-269970, a 5-HT₇ receptor antagonist, in mouse models predictive of antipsychotic-like activity. *Behav. Pharmacol.* **2008**, *19*, 153–159.
- (19) Leopoldo, M. Serotonin₇ receptors (5-HT₇Rs) and their ligands. *Curr. Med. Chem.* **2004**, *11*, 629–661.
- (20) Pittalà, V.; Salerno, L.; Modica, M.; Siracusa, M. A.; Romeo, G. 5-HT₇ receptor ligands: recent developments and potential therapeutic applications. *Mini Rev. Med. Chem.* **2007**, *7*, 945–960.
- (21) Hagan, J. J.; Price, G. W.; Jeffrey, P.; Deeks, N. J.; Stean, T.; Piper, D.; Smith, M. I.; Upton, N.; Medhurst, A. D.; Middlemiss, D. N.; Riley, G. J.; Lovell, P. J.; Bromidge, S. M.; Thomas, D. R. Characterization of SB-269970-A, a selective 5-HT₇ receptor antagonist. *Br. J. Pharmacol.* **2000**, *130*, 539–548.

- (22) Forbes, I. T.; Douglas, S.; Gribble, A. D.; Ife, R. J.; Lightfoot, A. P.; Garner, A. E.; Riley, G. J.; Jeffrey, P.; Stevens, A. J.; Stean, T. O.; Thomas, D. R. SB-656104-A: a novel 5-HT₇ receptor antagonist with improved in vivo properties. *Bioorg. Med. Chem. Lett.* **2002**, *12*, 3341–3344.
- (23) Kolaczowski, M.; Nowak, M.; Pawlowski, M.; Bojarski, A. J. Receptor-based pharmacophores for serotonin 5-HT₇R antagonists - implications to selectivity. *J. Med. Chem.* **2006**, *49*, 6732–6741.
- (24) Vermeulen, E. S.; Schmidt, A. W.; Sprouse, J. S.; Wikström, H. V.; Grof, G. J. Characterization of the 5-HT₇ receptor. Determination of the pharmacophore for 5-HT₇ receptor agonism and CoMFA-based modeling of the agonist binding site. *J. Med. Chem.* **2003**, *46*, 5365–5374.
- (25) Holmberg, P.; Sohn, D.; Leideborg, R.; Caldirola, P.; Zlatoidsky, P.; Hanson, S.; Mohell, N.; Rosqvist, S.; Nordvall, G.; Johansson, A. M.; Johansson, R. Novel 2-aminotetralin and 3-aminochroman derivatives as selective serotonin 5-HT₇ receptor agonists and antagonists. *J. Med. Chem.* **2004**, *47*, 3927–3930.
- (26) Paillet-Loilier, M.; Fabis, F.; Lepailleur, A.; Bureau, R.; Butt-Gueulle, S.; Dauphin, F.; Lesnard, A.; Delarue, C.; Vaudry, H.; Rault, S. Novel aminoethylbiphenyls as 5-HT₇ receptor ligands. *Bioorg. Med. Chem. Lett.* **2007**, *17*, 3018–3022.
- (27) Leopoldo, M.; Berardi, F.; Colabufo, N. A.; Contino, M.; Lacivita, E.; Niso, M.; Perrone, R.; Tortorella, V. Structure-affinity relationship study on *N*-(1,2,3,4-tetrahydronaphthalen-1-yl)-4-aryl-1-piperazinealkylamides, a new class of 5-HT₇ receptor agents. *J. Med. Chem.* **2004**, *47*, 6616–6624.
- (28) Leopoldo, M.; Lacivita, E.; Contino, M.; Colabufo, N. A.; Berardi, F.; Perrone, R. Structure-activity relationship study on *N*-(1,2,3,4-tetrahydronaphthalen-1-yl)-4-aryl-1-piperazinehexanamides, a class of 5-HT₇ receptor agents. 2. *J. Med. Chem.* **2007**, *50*, 4214–4221.
- (29) Hitchcock, S. A.; Pennington, L. D. Structure–brain exposure relationships. *J. Med. Chem.* **2006**, *49*, 7559–7583.
- (30) Pajouhesh, H.; Lenz, G. R. Medicinal chemical properties of successful central nervous system drugs. *NeuroRx* **2005**, *2*, 541–553.
- (31) van de Waterbeemd, H.; Camenisch, G.; Folkers, G.; Chretien, J. R.; Raevsky, O. A. Estimation of blood–brain barrier crossing of drugs using molecular size and shape, and H-bonding descriptors. *J. Drug Target.* **1998**, *6*, 151–165.
- (32) Chichak, K. S.; Peters, A. J.; Cantrill, S. J.; Stoddart, J. F. Nanoscale borromeates. *J. Org. Chem.* **2005**, *70*, 7956–7962.
- (33) Perrone, R.; Berardi, F.; Colabufo, N. A.; Lacivita, E.; Leopoldo, M.; Tortorella, V. Synthesis and structure–affinity relationships of 1-[ω -(4-aryl-1-piperazinyl)alkyl]-1-arylketones as 5-HT₇ receptor ligands. *J. Med. Chem.* **2003**, *46*, 646–649.
- (34) Leopoldo, M.; Berardi, F.; Colabufo, N. A.; Contino, M.; Lacivita, E.; Perrone, R.; Tortorella, V. Studies on 1-arylpiperazine derivatives with affinity for rat 5-HT₇ and 5-HT_{1A} receptors. *J. Pharm. Pharmacol.* **2004**, *56*, 247–255.
- (35) Caffieri, S. Reversed-phase high-performance liquid chromatography (RP-HPLC) determination of lipophilicity of furocoumarins. Relationship with DNA interaction. *J. Pharm. Sci.* **2001**, *90*, 732–739.
- (36) Compound **17** inhibited 62% binding of [³H]LSD at rat cloned 5-HT₇ receptor expressed in HEK-293 cells at concentration of 10⁻¹² M. The analysis of the *K_d* shift resulted in a linear plot with a slope significantly different from unity, which suggested an allosteric interaction between compound **17** and [³H]LSD under these experimental conditions. Binding experiments with compound **17** were also performed on human cloned 5-HT₇ receptor expressed in HEK-293 cells, yielding an apparent *K_i* value of 0.8 nM (*n_H* = 0.4). Compound **17** was also tested in the isolated guinea pig ileum assay used to evaluate the 5-HT₇ agonist-mediated relaxation of substance P-induced contraction. The response of compound **17** was identical to that of a 5-HT₇ receptor agonist (EC₅₀ = 4.50 mM). However, its effect was not abolished by the selective 5-HT₇ antagonist **2** at doses of 3, 5, and 10 mM. Also after 5-HT₇ receptor desensitization by 5-CT, compound **17** elicited relaxation at 2 and 3 mM and not at 1 mM. These data could indicate that compound **17** possess, at least in part, allosteric modulator properties on 5-HT₇ receptors. .
- (37) Faure, C.; Mnie-Filali, O.; Scarna, H.; Debonnel, G.; Haddjeri, N. Effects of the 5-HT₇ receptor antagonist SB-269970 on rat hormonal and temperature responses to the 5-HT_{1A/7} receptor agonist 8-OH-DPAT. *Neurosci. Lett.* **2006**, *404*, 122–126.
- (38) Monti, J. M.; Monti, D. The involvement of dopamine in modulation of sleep and waking. *Sleep Med. Rev.* **2007**, *11*, 113–133.
- (39) Caccia, S. N-dealkylation of arylpiperazine derivatives: disposition and metabolism of the 1-aryl-piperazines formed. *Curr. Drug Metab.* **2007**, *8*, 612–622.
- (40) Caccia, S. In-vivo metabolism of 4-substituted arylpiperazines to pharmacologically active 1-arylpiperazines. *Boll. Chim. Farm.* **1990**, *129*, 183–189.
- (41) Martin, G. E.; Elgin, R. J., Jr.; Mathiasen, J. R.; Davis, C. B.; Kesslick, J. M.; Baldy, W. J.; Shank, R. P.; DiStefano, D. L.; Fedde, C. L.; Scott, M. K. Activity of aromatic substituted phenylpiperazines lacking affinity for dopamine binding sites in a preclinical test of antipsychotic efficacy. *J. Med. Chem.* **1989**, *32*, 1052–1056.
- (42) Bantle, G. W.; Elworthy, T. R.; Guzman, A.; Jaime-Figueroa, S.; Lopez-Tapia, F. J.; Morgans, D. J.; Perez-Medrano, A.; Pfister, J. R.; Sjogren, E. B.; Talamas, F. X. Preparation of pyrimidinedione, pyrimidinetrione, triazinedione, and tetrahydroquinazolinone derivatives as α -1-adrenoceptor antagonists. Eur. Pat. Appl. 748800, 1996; *Chem. Abstr.* **1996**, *126*, 131468.
- (43) Jasper, J. R.; Kosaka, A.; To, Z. P.; Chang, D. J.; Eglén, R. M. Cloning, expression and pharmacology of a truncated splice variant of the human 5-HT₇ receptor (h5-HT_{7b}). *Br. J. Pharmacol.* **1997**, *122*, 126–132.
- (44) Fargin, A.; Raymond, J. R.; Regan, J. W.; Cotecchia, S.; Lefkowitz, R. J.; Caron, M. G. Effector coupling mechanisms of the cloned 5-HT_{1A} receptor. *J. Biol. Chem.* **1989**, *264*, 14848–14852.
- (45) Scarselli, M.; Novi, F.; Schallmach, E.; Lin, R.; Baragli, A.; Colzi, A.; Griffon, N.; Corsini, G. U.; Sokoloff, P.; Levenson, R.; Vogel, Z.; Maggio, R. D₂/D₃ dopamine receptor heterodimers exhibit unique functional properties. *J. Biol. Chem.* **2001**, *276*, 30308–30314.
- (46) Carter, D.; Champney, M.; Hwang, B.; Eglén, R. M. Characterization of a postjunctional 5-HT receptor mediating relaxation of guinea pig isolated ileum. *Eur. J. Pharmacol.* **1995**, *280*, 243–250.
- (47) *PowerLab/400 (version for Windows)*; ADInstruments Pty Ltd.: Castle Hill, Australia.
- (48) de Boer, V. C.; Dihal, A. A.; van der Woude, H.; Arts, I. C.; Wolffram, S.; Alink, G. M.; Rietjens, I. M.; Keijer, J.; Hollman, P. C. Tissue distribution of quercetin in rats and pigs. *J. Nutr.* **2005**, *135*, 1718–1725.
- (49) *GraphPad Prism Software (version for Windows)*; GraphPad Software, Inc.: San Diego, CA.
- (50) Cheng, Y. C.; Prusoff, W. H. Relationship between the inhibition constant (*K_i*) and the concentration of inhibitor which causes 50% inhibition (IC₅₀) of an enzymatic reaction. *Biochem. Pharmacol.* **1973**, *22*, 3099–3108.
- (51) *ClogP 4.0 (version for Windows)*; BioByte Corp.: Claremont, CA.

JM800615E